

Diagnosing the velocity-space separatrix of trapped particle modes

A. A. Kabantsev^{a)} and C. F. Driscoll

Physics Department, University of California, San Diego, California 92093-0319

(Presented on 9 July 2002)

Trapped particle modes in pure electron plasmas are similar to modes in neutral plasmas and exhibit damping due to velocity diffusion across the separatrix between trapped and untrapped particles, as commonly occurs in neutral plasmas. Applied rf voltages cause resonant perturbation of particle velocities near the separatrix, giving a greatly enhanced mode damping. This diagnostic technique can determine the velocity-space separatrices for either electrostatic or magnetic trapping, or determine the particle distribution function along the separatrix. © 2003 American Institute of Physics. [DOI: 10.1063/1.1534902]

I. INTRODUCTION

Trapped-particle modes are well-established features of magnetically confined plasmas¹⁻⁴ but they are rarely used for primary diagnostic purposes. The recently discovered trapped-particle $\mathbf{E} \times \mathbf{B}$ drift modes⁵ in non-neutral plasmas represent an intriguing new class of plasma modes which enable direct manipulation and detection of the velocity-space separatrix between trapped and untrapped particles. Here, we give a brief review of these modes in pure electron plasmas with electrostatic or magnetostatic trapping, and demonstrate resonant velocity diffusion of particles across the velocity-space trapping separatrix. For electrostatic trapping, this technique clearly identifies the magnitude of the trapping potential in the plasma; and for magnetic trapping it gives the pitch angle of the separatrix or the particle distribution function along it.

In general, electrostatic and magnetic field inhomogeneities in confinement devices cause a fraction of the particle distribution $f(v_{\parallel}, v_{\perp})$ to remain localized in z , i.e., along the trap axis, so velocity-space separatrices between trapped and passing particles are commonplace in confined plasmas. Interactions between these trapped and untrapped particles often sustain collective trapped particle modes (or instabilities), which then can also affect the global transport rate. Here, passing particles move along magnetic field lines adiabatically in response to a potential perturbation, while trapped particles remain isolated from the global mode structure and $\mathbf{E} \times \mathbf{B}$ drift across field lines locally. These different types of motion executed by the trapped and passing fractions lead to a sharp discontinuity in the particle distribution function. This discontinuity means that even small angle scattering near the velocity-space separatrix can cause detrapping, and this separatrix mixing determines the trapped particle mode damping.⁶

Normally, particles diffuse through the separatrix due to binary Coulomb collisions, which are relatively rare events in “collisionless” high-temperature or/and low-density plasmas. However, a greatly enhanced scattering through the separatrix can be deliberately induced by applying rf-drive in

resonance with axial bounce motion of the marginally trapped particles. This deliberately enhanced scattering immediately causes readily measurable effects, such as increased mode damping and increased global transport rate. Using this technique as a diagnostic tool in pure electron plasmas, we have traced the separatrix in velocity space both for electrically and magnetically trapped particles.

II. EXPERIMENTAL SETUP

The experiments are performed on quiescent pure electron plasmas contained in a cylindrical Penning–Malmberg trap,^{5,7} shown in Fig. 1. The plasma column of total length $L_p \approx 48$ cm is contained inside conducting cylinders of radius $R_w = 3.5$ cm, which reside in an ultrahigh vacuum with $P \approx 10^{-10}$ Torr. The end electrodes are negatively biased, thereby providing axial confinement. A strong axial magnetic field ($B \lesssim 10$ kG) provides radial confinement. The electron plasma is generated by thermionic emission from a hot tungsten filament. The electron columns typically have central densities $1 \lesssim n_0 \lesssim 2 \times 10^7$ cm⁻³ over a radius of $R_p \approx 1.2$ cm, with thermal energies $0.5 < T < 6$ eV. The unneutralized electron charge results in a central potential $-\phi_0 \approx -30$ V, and the radial electric field causes $\mathbf{E} \times \mathbf{B}$ drift rotation around an axis through the center of charge, at a rate $0.02 \lesssim f_E \lesssim 0.2$ MHz. Typical profiles of $n(r)$ and $f_E(r)$ are shown in Fig. 2.

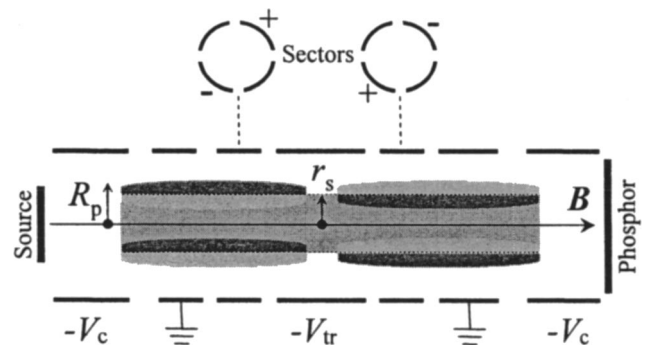


FIG. 1. Cylindrical trap electrodes and plasma column with central barrier V_{tr} and density variations representing the $m_{\theta} = 1$ z -asymmetric trapped particle mode.

^{a)}Electronic mail: aakpla@physics.ucsd.edu

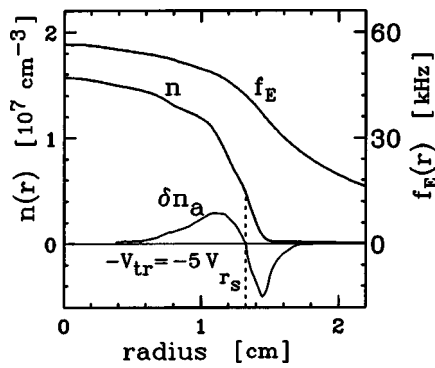


FIG. 2. Measured plasma density $n(r)$ and resulting $\mathbf{E} \times \mathbf{B}$ rotation $f_E(r)$ at $B=4$ kG. Also shown is the radial eigenfunction $\delta n_a(r)$ for the trapped particle mode.

This rotation frequency tends to be substantially less than the axial bounce frequency for thermal electrons, which is

$$f_b \equiv (T/m)^{1/2}/2L_p \approx 0.5 \text{ MHz}. \quad (1)$$

The apparatus is operated in inject-manipulate-dump cycles, and has a shot-to-shot reproducibility of $\delta n/n \leq 1\%$. The bounce-averaged radial profile of electron density can be measured (destructively) at any time by dumping the electrons axially onto a phosphor screen imaged by a charge coupled device camera.⁷ Taking these images at consecutive times, we obtain the bulk transport rate, $v_P(t)$, defined as normalized rate of change of the plasma mean square radius, i.e.,

$$v_P \equiv \frac{d}{dt} \langle r^2 \rangle / \langle r^2 \rangle. \quad (2)$$

The plasma is heated by applying short rf bursts of variable amplitude and frequency to one of the end confining cylinders in resonance with thermal particle bounce motion,⁸ and the plasma temperature is measured using a standard dynamic-evaporation technique.⁹

III. TRAPPED PARTICLE MODES

The simplest and most controllable trapped particle states are obtained by applying a voltage V_{tr} to a ring electrode near the axial center of the plasma column. This creates a barrier (localized in z) which decreases in strength as $r \rightarrow 0$. Particles with high parallel velocities pass through the barrier region and sample the entire length of the plasma column during their bounce motion, while particles with low parallel velocities are effectively trapped in local regions separated by the barrier. Alternately, a localized increase in magnetic field from B to $B + \delta B$ could form a magnetic barrier, with a substantially different velocity-space separatrix, as shown in Fig. 3. Magnetic trapping also introduces weak electrostatic potential variations along the magnetic field lines, altering the separatrix at low velocities,¹⁰ but the (subtle) effects of these potential variations have not yet been measured.

Trapped particle modes arise because the trapped and passing particles experience different bounce-averaged $\mathbf{E} \times \mathbf{B}$ drifts. A collective motion occurs in which the trapped and

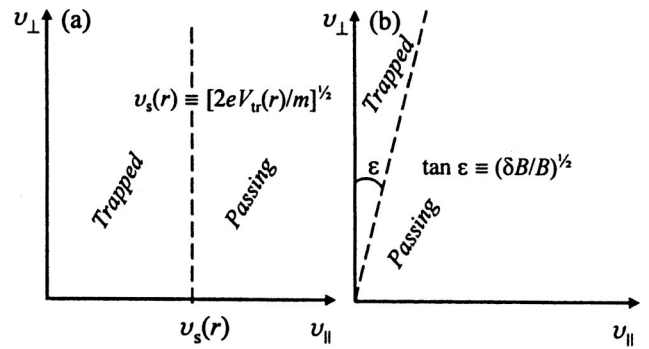


FIG. 3. Idealized velocity-space separatrices for (a) electrostatic and (b) magnetostatic trapping.

passing fractions oscillate “against” each other at frequency $f_a \lesssim f_E$, i.e., when the passing particles respond adiabatically to the potential perturbations created by the displacement of the trapped particles. The simple $m_\theta=1$, trapped particle mode which arises from an applied V_{tr} has (predominantly trapped) $\mathbf{E} \times \mathbf{B}$ drifting particles for $r > r_s$, Debye shielded by (predominantly passing) particles for $r < r_s$. Overall, the mode has density perturbations

$$\delta n_a = \delta n_a(r) \cos(\theta) \text{sign}(z) \exp\{i2\pi f_a t - \gamma_a t\}. \quad (3)$$

The mode is asymmetric (not sinusoidal) across $z=0$, so the passing particles experience no net $\mathbf{E} \times \mathbf{B}$ drift. The measured eigenfunction $\delta n_a(r)$ in Fig. 2 changes sign for $r < r_s$, demonstrating “shielding” of the perturbations at $r > r_s$.

This trapped particle mode is damped by collisions which cause velocity-space diffusion across the separatrix between trapped and passing particles. The 90° scattering rate in these plasmas is $v_{ee} \approx 100 \text{ s}^{-1}$; however, the effective scattering across the separatrix is substantially greater.⁶ The different dynamics executed by the trapped and passing particles tends to produce a sharp discontinuity in the distribution functions near the separatrix velocity. Nevertheless, a Fokker-Planck analysis of collisional diffusion yields damping rates which are in close agreement with experiment.¹¹

We note that the frequency ordering for these modes, i.e.,

$$f_b \gg f_a \approx f_E \gg v_{ee} \quad (4)$$

is the same as commonly found for trapped particle modes in fusion-oriented plasmas. However, there is no driving mechanism for instability in single-species plasmas, so the modes can be precisely characterized with controlled experiments.

IV. DIAGNOSING THE SEPARATRIX

This mode damping can be greatly enhanced by applying an external rf drive that is resonant with the axially bouncing marginally trapped particles, as shown in Fig. 4. The mode is first excited (by sinusoidal wall voltages at $f_a = 26.55$ kHz), then decays naturally with damping rate $\gamma_a = 535 \text{ s}^{-1}$. Applying an 0.2 V rf wiggle at $f_{rf} = 1.6$ MHz to one containment cylinder causes an immediate tenfold increase in damping to $\gamma_a = 5350$. Here, the resonant particles are at v_s

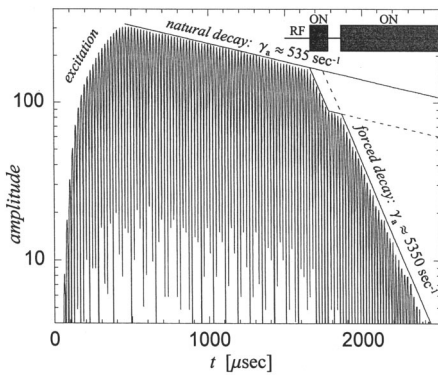


FIG. 4. Trapped particle mode excitation, natural decay, and enhanced decay due to rf-induced scattering across the separatrix.

$=f_{rf} \cdot L_P$, and the enhanced damping occurs only when the rf is on, since there is little bulk plasma heating.

Observing the mode damping while varying the rf drive frequency allows us to map out the range of separatrix velocities, as shown in Fig. 5. The rf is resonant with particles having $v_{||} = f_{rf} L_P$, and enhanced damping occurs when this corresponds to the separatrix velocity at some radius, i.e., $v_s(r) = f_{rf} L_P$. The total scattering across the separatrix is apparently weighted by the product $n_{tr}(r) \cdot n_{pas}(r)$ of trapped and passing particle fractions, so there is some effective radially averaged separatrix velocity v_s^* .

The damping enhancement of Fig. 5 shows a peak at f_{rf}^* , with a Gaussian shape for which we have no accurate model. We find that f_{rf}^* appropriately scales inversely with plasma length L_P , and shows no dependence on magnetic field B . The peak frequency f_{rf}^* probes separatrix velocities v_s^* corresponding to barrier heights $eV_s^* = 0.46$ eV for plasmas with $T = 0.6$ eV and $eV_s^* = 0.87$ eV for $T = 6$ eV. There is a weak temperature dependence which represents the change in Debye shielding of the externally applied trapping voltage. At fixed temperature, the peak frequency scales with applied trapping voltage as $f_{rf}^* \propto V_{tr}^{1/2}$, as expected. In resonance, the measured magnitude of this enhancement depends linearly on the amplitude V_{rf} of the rf drive (see Fig. 6), and it is independent of electron temperature T , so long as $V_{rf} \lesssim k_B T / e$. Additionally, we typically observe several reso-

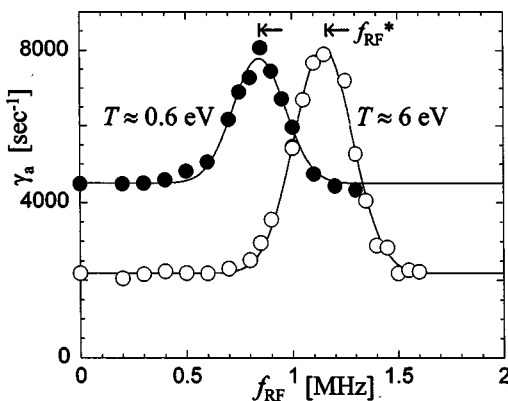


FIG. 5. Trapped particle mode damping rate γ_a vs frequency f_{rf} causing enhanced velocity scatterings across the separatrix.

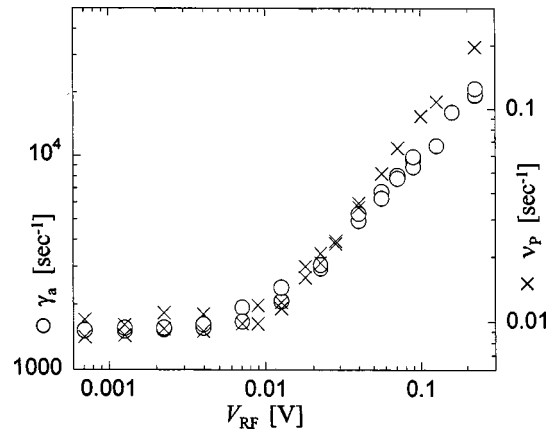


FIG. 6. The measured bulk plasma expansion rate ν_p increases proportional to the measured trapped particle mode damping γ_a as the rf drive increases separatrix scatterings.

nances of higher order, since the width of the primary resonance is small compared to the resonant frequency.

V. ASYMMETRY-INDUCED TRANSPORT

These trapped particle modes and their dissipative damping are central to the bulk radial particle transport which occurs due to the inevitable small θ asymmetries in the trap containment fields. For example, an overall misalignment of $\alpha = 0.2$ mrad between B and the axis of the cylindrical electrodes typically causes a measurable bulk expansion, with a rate $\nu_p \sim 10^{-2} \text{ s}^{-1}$ at $B = 1$ kG, due to naturally occurring electric and magnetic trapping. This bulk expansion rate is found to be proportional to the damping rate γ_a of the trapped particle mode and to the number of trapped particles. Applying a (θ symmetric) voltage $-V_{tr} = -4$ V allows us to control the number of trapped particles and the mode characteristics. Figure 6 shows this proportionality between ν_p and γ_a as γ_a is increased tenfold through application of V_{rf} at the separatrix-resonant frequency f_{rf}^* . Fully characterizing this connection between trapped particle modes and bulk particle transport remains an exciting challenge.¹²

VI. MAGNETIC TRAPPING

Magnetic trapping barriers are similar in effect to these electrostatic barriers, although the velocity-space separatrix is qualitatively different, as shown in Fig. 3. Moreover, the experimental apparatus does not yet have a separately controlled magnetic barrier, so our magnetic trapping results were obtained from inherent magnetic field ripples. These ripples have magnitude $\delta B/B \approx 10^{-3}$, with an axial extent of about 25 cm. Even these small ripples cause a considerable fraction (3%) of the plasma electrons to be trapped axially.

The trapped particle modes from these small magnetic ripples are too weak for accurate measurements of the damping rate γ_a ; but the mode and its damping are still directly reflected in the bulk plasma expansion rate ν_p . For example, Fig. 7 shows the enhancement in the measured ν_p as an rf drive is applied to enhance velocity scatterings across the magnetic separatrix. Here, there are two small magnetic maxima in the plasma region, and V_{rf} is applied in the region

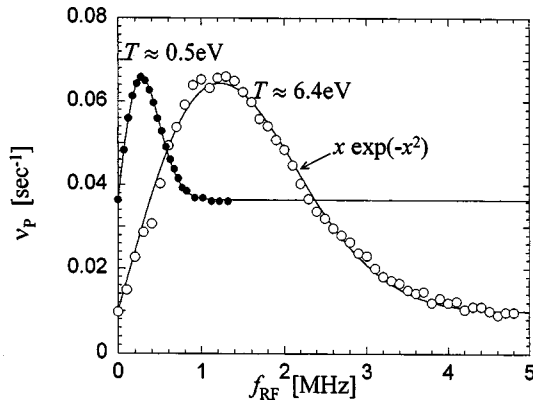


FIG. 7. For (weak) magnetic trapping, the variation of the expansion rate ν_p with f_{rf} accurately reflects the Maxwellian distribution of particles at the separatrix for two different plasma temperatures T .

of a magnetic minimum. Electrons receive a sharp, nonadiabatic kick if they have $v_{\parallel} \approx L^* f_{rf} \ll \bar{v}$, where $L^* \equiv 2R_w/j_{01}$ is the axial extent of the electric fields from the applied rf drive. Here, we have used the “sheath transit” resonance to interact with particles with small v_{\parallel} , while still keeping $f_{rf} > f_E$.

The enhancement in the transport rate $\Delta \nu_p$ is due to an enhancement in the trapped particle mode damping, which is proportional to the velocity space density $v_{\perp} f_e(v_{\parallel}, v_{\perp})$ of resonant electrons in a boundary layer determined by the separatrix ratio $v_{\parallel}/v_{\perp} = (\delta B/B)^{1/2} \equiv \tan \varepsilon$ and by the resonance condition $v_{\parallel} = L^* f_{rf}$. For a Maxwellian distribution, this gives

$$\Delta \nu_p = A x \exp(-x^2),$$

with

$$x \equiv (\sqrt{2} R_w / j_{01} \varepsilon \bar{v}) f_{rf}. \quad (5)$$

With $\varepsilon = 0.03$ known from the magnetic ripple strength, fitting the frequency-response curves of Fig. 7 to Eq. (5) directly gives the two free parameters A and $\bar{v} \equiv \sqrt{T/m}$. The fits are surprisingly accurate, giving the (separately measured) plasma temperature T to within 10%, and suggesting

that the distribution function is indeed closely Maxwellian. Alternately, this fit with a known T would give the magnitude of the field ripples ε . Thus the diagnostic information gained in the magnetic case is more incisive, since the magnetic separatrix is nontrivial. Of course, these magnetic trapping effects will be apparent only when electrostatic trapping (if present) is weak enough that $v_s^* \ll \varepsilon \bar{v}$.

VII. CONCLUSION

In conclusion, trapped particle modes arise even with small electric or magnetic containment field ripples. The damping of these modes arises from scattering across the velocity-space trapping separatrix and is intimately connected to asymmetry induced bulk particle transport. We find that an applied rf drive causes resonant enhancement of these scatterings, thereby increases the damping (and transport) rates, and offers a direct probe of the separatrix or of the particle distribution function.

ACKNOWLEDGMENTS

This work was supported by Office of Naval Research Grant No. ONR N00014-96-1-0239 and National Science Foundation Grant No. PHY-9876999.

- ¹B. B. Kadomtsev and O. P. Pogutse, Sov. Phys. JETP **24**, 1172 (1967).
- ²G. A. Navratil, A. K. Sen, and J. Slough, Phys. Fluids **26**, 1044 (1983).
- ³H. P. Warren and M. E. Mauel, Phys. Rev. Lett. **74**, 1351 (1995).
- ⁴G. Vetoulis and M. Oppenheim, Phys. Rev. Lett. **86**, 1235 (2001).
- ⁵A. A. Kabantsev, C. F. Driscoll, T. J. Hilsabeck, T. M. O’Neil, and J. H. Yu, Phys. Rev. Lett. **87**, 225002 (2001).
- ⁶M. N. Rosenbluth, D. W. Ross, and D. P. Kostomarov, Nucl. Fusion **12**, 3 (1972).
- ⁷K. S. Fine, W. G. Flynn, A. C. Cass, and C. F. Driscoll, Phys. Rev. Lett. **75**, 3277 (1995).
- ⁸B. P. Cluggish, J. R. Danielson, and C. F. Driscoll, Phys. Rev. Lett. **81**, 353 (1998).
- ⁹D. L. Eggleston, C. F. Driscoll, B. R. Beck, A. W. Hyatt, and J. H. Malmberg, Phys. Fluids B **4**, 3432 (1992).
- ¹⁰R. Goplan, Ph.D. thesis, University of California, Berkeley, CA, 1998; J. Fajans (to be published).
- ¹¹T. J. Hilsabeck and T. M. O’Neil, Bull. Am. Phys. Soc. **47**, 125 (2002).
- ¹²A. A. Kabantsev and C. F. Driscoll, Phys. Rev. Lett. **89**, 245001 (2002).